scientific reports

Check for updates

OPEN

Rapid CO_2 mineralization by zeolite via cation exchange

Abdulwahab Alqahtani✉, Mouadh Addassi, Hussein Hoteit & Eric Oelkers

This study illuminates the mineral carbonation potential of zeolite minerals. Zeolite minerals are common alteration products of basaltic rocks and are known for their ability to rapidly exchange their interstitial cations with those in aqueous solutions. A series of closed system batch reactor experiments was conducted at 60 °C by combining stilbite, a Ca-bearing zeolite, with 0.1 mol/kg_w aqueous sodium carbonate solutions. The individual batch reactor experiments ran from 2 to 225 days. Scanning electron microscope images of the solids recovered from the experiments reveal the presence of extensive calcite crystals, suggesting rapid and efficient carbonation. The total mass of CO_2 mineralized during the experiments, determined from the direct analysis of the solids by thermogravimetric analysis and organic carbon analysis, equaled more than 5% of that of the original stilbite within a month. This is approximately equal to maximum CO_2 mineralization possible if all of the Ca in the original stilbite was incorporated into calcite. Chemical analysis of reacted stilbite shows that approximately 2 Na atoms were incorporated into stilbite for each Ca atom incorporated into the precipitated calcite. These observations indicate that the carbon removal by stilbite proceeded by the rapid exchange of Na for Ca in its structure. This process results in carbonation rates that are far faster than those achieved by a silicate dissolution-carbonate precipitation mechanism. These results, consequently, compel consideration of targeting subsurface mineral carbonation efforts into zeolite-rich rocks.

Keywords CO_2 mineralization, CCUS, Mineral carbonation, CO_2 storage, Zeolites, Carbon capture and storage

Carbon dioxide mineralization is the process by which CO_2 is transformed into stable carbonate minerals through its reaction with Ca- and/or Mg-rich silicates[1–6]. This carbon removal process has received increased interest as several studies have demonstrated that mineral carbonation is a safe and effective method for the long-term disposal of carbon dioxide[5,7,8]. Mafic and ultramafic rocks are commonly considered the most suitable host rocks for subsurface carbon mineralization due to their abundance in divalent cations (e.g., Ca^{2+}, Mg^{2+}, Fe^{2+}) and relatively high reactivity[9–11,5,12,13]. Optimizing the rate and extent of mineral carbonation for the purpose of carbon disposal is facilitated by knowledge of the carbonation rates of the individual minerals[14,15].

A number of studies have concluded that the overall rate of CO_2 mineralization in mafic and ultramafic rocks is limited by the release rate of divalent metal cations to the fluid phase[16–19]. For many minerals, the release of divalent metal cations requires mineral dissolution. A faster process of releasing divalent metals to aqueous solutions, and one that has been thus far largely overlooked in terms of carbon mineralization, is cation exchange. Cation exchange is observed in a number of minerals, notably clay minerals, including smectite, vermiculite, allophane, and zeolites[20]. The presence of these minerals may, therefore, make them favorable for carbon storage through mineral carbonation.

Among these minerals, the zeolites may provide excellent opportunities for mineral carbonation. Zeolite minerals are found in some sedimentary rocks, volcanic terrains, and in some oil and gas reservoirs[21–24]. The cations in natural zeolite exchange sites are commonly Ca-rich[25]. Notably, zeolites are abundant in some of the rocks being considered for subsurface mineral storage, including in Iceland, India, and Georgia[12,26,27].

The purpose of this study is to assess the potential of zeolite minerals to promote carbon dioxide disposal through mineral carbonation. Towards this goal, we have reacted the common zeolite, stilbite, in closed system experiments at 60 °C in the presence of aqueous 0.1 mol/kg $NaCO_3$ solutions. Stilbite was selected for this study as it is one of the most common natural zeolites[28,29], and due to the dominance of Ca as the exchangeable cation in the structure of most natural stilbites[30]. The purpose of this paper is to report the results of stilbite carbonation experiments and to apply these results to the improved mineral storage of CO_2 in subsurface systems.

Physical Science and Engineering Division, King Abdullah University of Science and Technology (KAUST), Thuwal 23955, Saudi Arabia. ✉email: abdulwahab.alqahtani@kaust.edu.sa

Background

Zeolites are a group of naturally occurring minerals mainly comprised of silicon, aluminum, oxygen, and metal cations[22,23]. The structure of zeolite minerals consists of Si-O and Al-O tetrahedra linked together in polyhedra[31]. Zeolites are used in various applications, including water purification, catalysis, and as CO_2 adsorbents[32–35]. They are characterized by their open microporous structure with large, interconnected cages within their framework[33], as shown in Fig. 1. These cages are filled with water molecules and exchangeable cations. The cages in zeolite structure can be sufficiently large to allow for the exchange of two monovalent cations for one divalent cation and vice-versa in accord for example with the reaction[36].

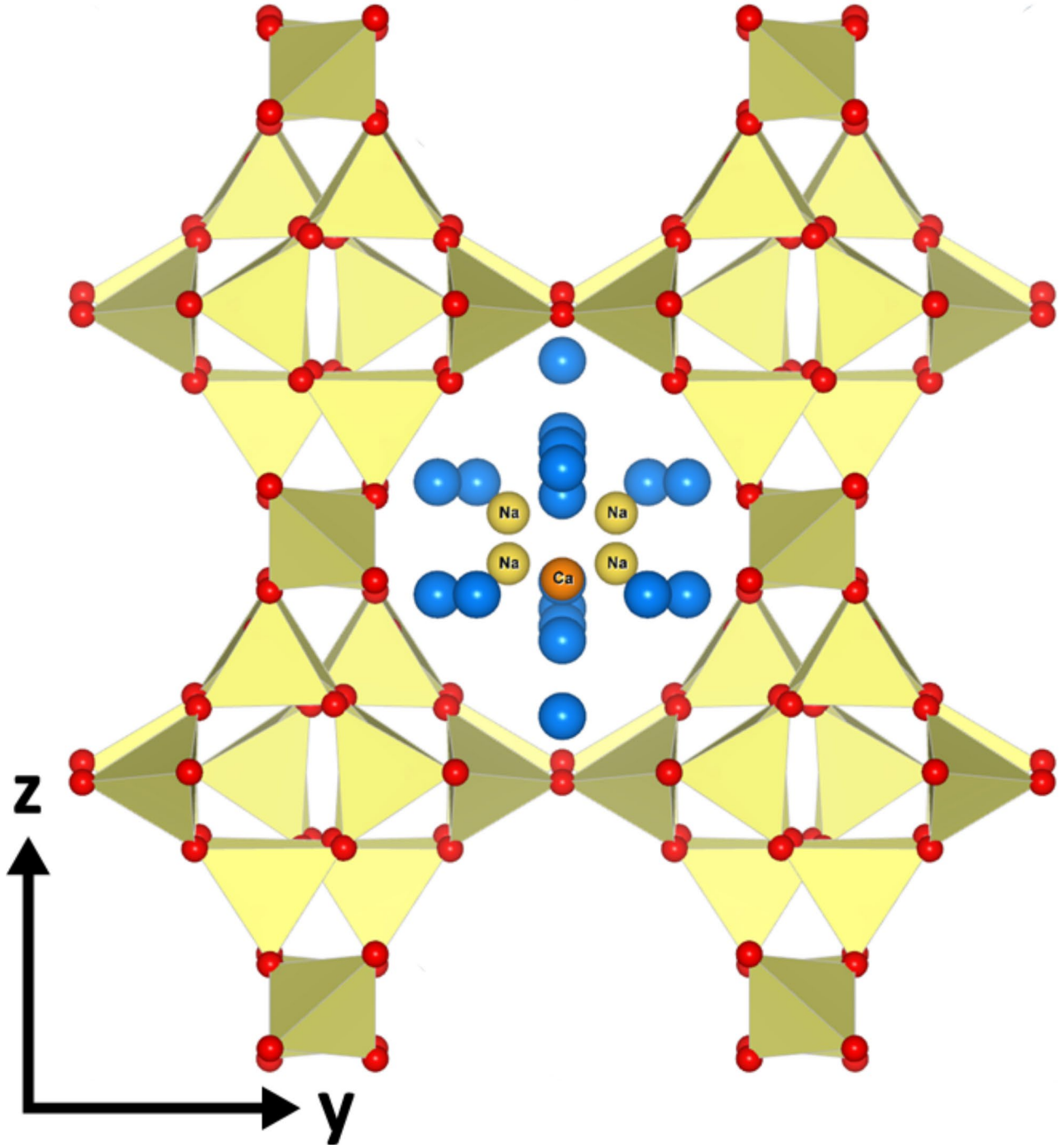

Fig. 1. Stilbite structure displaying its silicate and aluminate tetrahedra in yellow, forming a distinctive open framework with interconnected channels. The red dots represent oxygen atoms at the tetrahedra's vertices. Calcium and sodium atoms and water molecules, depicted in orange, yellow, and blue spheres, respectively, occupy the channels, facilitating ion exchange and water retention[42].

$$NaCa_4Al_9Si_{27}O_{72} + 2Na^+ \leftrightarrow Na_3Ca_3Al_9Si_{27}O_{72} + Ca^{2+} \quad (1)$$

This exchange can be rapid and extensive[37,38]. Curkovic et al.[39] observed a substantial exchange of 1 Ca for 2 Na in 0.1 to 2 mm-sized heulandite grains in contact with 2 M aqueous NaCl solutions at 22 °C within 24 h. This exchange proceeds by the coupled diffusion of cations into and out of the zeolite structure without otherwise disrupting the Si-Al-O framework of this mineral[40]. In the case of stilbite, a nearly complete exchange of Ca for Na has been observed in natural samples placed in continuous contact with aqueous 1 M NaCl solutions at 100 °C for 16 days[41].

Once divalent calcium is released into the fluid phase, it could readily react with aqueous bicarbonate or carbonate to form stable calcite, for example, in accord with

$$Ca^{2+} + CO_3^{2-} \leftrightarrow CaCO_3\,(\text{calcite}) \quad (2)$$

The combination of reactions (1) and (2) could lead to the mineral storage of CO_2 without the need to rely on relatively slow silicate mineral dissolution reactions.

Several studies have reported measured dissolution rates, based on Si release, of zeolite minerals[43–46]. For example, Ragnarsdóttir[45] reported the dissolution rates of the heulandite measured over a large range of pH at ambient temperature. The dissolution rate of scolecite, a Ca-bearing zeolite, was studied by Heřmanská et al.[46]. To our knowledge, this study is the first to focus on quantifying directly the carbonation rates of zeolite minerals.

Methods

Stilbite powders

The stilbite sample used in this study was obtained from the Alex Kalber collection of the Icelandic Institute of Natural History. It was originally sampled from Melshorn Mountain, part of the Tertiary basalt formations of Eastern Iceland. The stilbite sample was broken into smaller pieces using a laboratory jaw crusher. The crushed sample was then ground with an agate mortar and pestle and sieved to recover the 40–150 µm size fraction. The recovered ground stilbite was cleaned multiple times using acetone in an ultrasonic bath to remove ultra-fine particles. Acetone was chosen because, although it may temporarily displace water from the hydrophilic pores of natural zeolites, it does not chemically alter the surface. The structure rehydrates readily upon exposure to moisture[47], and any residual acetone evaporates quickly during the drying process. The sample was then dried in a 40 ^{0}C drying oven for five days. The surface area of the dried prepared stilbite powder (SSA) was measured using Micromeritic Instruments ASAP-2420, following the multi-point nitrogen gas physisorption analysis at 77 K, according to the Brunauer-Emmett-Teller (BET) method[48]. The SSA determined for the stilbite was 0.10 ± 0.002 m^2/g. The identity of this powder was confirmed by measuring its X-ray diffraction (XRD) pattern using a Bruker D2 PHASER. XRD scanning was conducted in the range of 5–70° (2θ) at the rate of 1° (2θ) per second. The prepared powders were further analyzed by scanning electron microscope (SEM) using a FE-SEM Thermo Fisher Teneo with an acceleration voltage ranging between 3 and 20 kV. This SEM is equipped with a 150 mm Oxford XMax detector for elemental analysis via energy-dispersive X-ray spectroscopy (EDS).

Batch-reactor experiments

Stilbite carbonation experiments were performed as a series of individually sealed closed system batch experiments in 50mL CentriStar polypropylene sterile, airtight vessels. Five individual batch reactor experiments were conducted at 60 °C and ambient pressure of ~1 bar. The experiments were initiated by placing 0.3 g of prepared ground stilbite and 30 g of initial reactive fluid in each polypropylene batch reactor. These reactors were then sealed individually to isolate them from the atmosphere. The initial reactive fluids were comprised of 0.1 mol/kg ACS reagent grade sodium carbonate (Na_2CO_3) and ultra-pure deionized water. The initial 21 °C pH of this fluid was 11.48. The prepared reactors were placed in a Jeio Tech brand IS-971RF shaking temperature-controlled incubator. This incubator ensures particle suspension within the reactors at a stable temperature.

Each batch reactor remained sealed until a preselected time. These times were chosen to observe and quantify the temporal evolution of the carbonation reactions. At each selected time, the fluids and solids were collected from a reactor and separated for subsequent analysis. The fluid samples were divided into two subsets; one was used for pH measurement, and the other was acidified with 1% ultrapure nitric acid (HNO_3) for elemental analysis. The solids from the batch reactors were collected by vacuum filtration using 3 µm ashless high-quality cotton filters. The collected solids were then stored in an oven at 40 °C for approximately one week before post-experiment analysis.

Analytical and computational analyses

The elemental composition of the initial stilbite powder was determined by X-ray fluorescence (XRF) using a Bruker S8 TIGER Wavelength Dispersive X-Ray Fluorescence (WDXRF) spectrometer. This spectrometer employs the GEO-QUANT analytical method for processing XRF data. The method is designed for the analysis of major and minor oxides in geological materials and uses optimized calibration models and matrix corrections for improved accuracy. To prepare a fused bead for analysis, the unreacted stilbite was finely ground and homogenized with a lithium borate flux at a 1:10 sample-to-flux ratio. The mixture was then placed in a platinum crucible and heated to over 1000 °C, producing a clear, glassy bead suitable for precise XRF analysis upon cooling. The fusion method provides a highly homogeneous material and minimizes uncertainty. The

overall uncertainty of the XRF measurements generally depends on the calibration, the standards used, and the sample preparation. The estimated uncertainty of each analysis is provided together with the XRF results in the Results section. The solids recovered after the experiments were not analyzed using XRF due to the limited amount of available material.

The major element compositions of the reactive fluids were measured using an Agilent 5110 inductively coupled plasma-optical emission spectrometer (ICP-OES). This instrument was calibrated using standard solutions with concentrations similar to those of the reactor fluids. The elemental composition of post-experiment solid samples was also analyzed using the ICP-OES. Prior to elemental analysis, 30 mg of each solid sample was digested in a mixture of 1 ml of 48% hydrofluoric (HF) acid, 1 ml of 37% hydrochloric (HCl) acid, and 3 ml of 70% nitric acid. The solid-fluid mixture was then placed in an incubated shaker at 60 °C for 2 h to completely dissolve the solids. The resulting solutions were cooled and diluted to a total volume of 50 ml using ultra-pure deionized water. The ICP-OES measurement uncertainties range between 5 and 12% depending on the element analyzed. These uncertainties are based on the replicate measurement of certified standard solutions. The pH of the collected reactive fluid samples was measured using a Fisherbrand™ accumet™ Basic AB315 meter. The pH electrodes were calibrated using 4.01 and 9.21 pH buffer solutions at 21 °C. The accuracy of the pH measurements was determined to be ±0.05 based on repeated analyses. The in-situ pH at the experimental temperature of 60 °C was calculated using the PHREEQC together with measured 21 °C pH and elemental compositions.

Thermogravimetric Analysis (TGA) was performed on the pre- and post-experiment solids using a TA Discovery 650 Thermal Analyzer coupled with a Quadrupole Mass Spectrometer (QMS). This analysis provides the mass of CO_2 liberated from the solids phases as the sample is heated, as well as the ion current of H_2O and CO_2 to confirm the source of the mass loss. In this way, TGA provides the mass of CO_2 present either as a mineral or adsorbed to a solid phase. The H_2O and CO_2 ion current analysis ensures the reliability of this method, particularly for natural zeolites, which can exhibit distinct thermal behaviors due to variations in their cation composition and water arrangements[47,49]. An amount of 10 mg of each stilbite sample was used for each TGA analysis. The uncertainty from this approach originates from several factors, including the precision of the TGA and the representativeness of the 10 mg sample used in the TGA analysis. This latter source of uncertainty was limited by grinding and mixing each sample prior to analysis. The estimated uncertainties of these analyses are presented in the Results section. A Thermo Fisher Flash 2000 Organic Elemental Analyzer (OEA) was also used to determine the mass of CO_2 in the pre- and post-experiment solids.

Geochemical speciation calculations were performed to determine the saturation indices of selected minerals. These calculations were performed utilizing the PHREEQC software[50,51] together with its 'kinec.dat' database[43,52,53].

Results

Temporal evolution of reactive fluids

In total, five batch-reactor experiments were performed. Table 1 reports the compositions of the fluids recovered from the experiments. The initial reactive fluid pH at 60 °C was 10.7. The pH of the reactive fluids, as shown in Fig. 2, decreases slightly to 10.4 over approximately 200 days. Figure 2 also shows the temporal concentration evolution of dissolved Al, Ca, and Si in the reactive fluids. The concentration of dissolved calcium increased due to fluid-stilbite interactions but did not exceed 3×10^{-5} mol kg^{-1}in the experiments. The total Ca in the reactive fluids did not exceed 0.21% of the original Ca mass in the unreacted stilbite. A relatively rapid increase in reactor fluid Si concentration is seen at the beginning of the experimental series; this concentration is then observed to stabilize at approximately 1×10^{-3} mol kg^{-1}. A similar behavior is observed for Al, where its concentration initially increased during the first 50 days, then it leveled off at 2.3×10^{-4} mol kg^{-1}.

The saturation indices of selected minerals with respect to the reactive fluid are depicted in Fig. 3. The reactive fluids are close to equilibrium with respect to calcite, magnesite, and dolomite throughout the experimental series. Stilbite remains undersaturated throughout the experimental series, suggesting that the mineral could dissolve continuously. The saturation indices of Na-rich zeolites approach equilibrium after 50 days of reaction, while those of the Ca-rich zeolites remain undersaturated. Mg-saponite clay was supersaturated in the reactive

Sample	Elapsed time [days]	Fluid pH		Element concentration in the reactor fluids [mol/kg_w]			
		at 21 °C	at 60 °C	Al	Ca	Mg	Si
Unreacted	0	11.48	10.56	0	0	0	0
S1	2	11.3	10.45	1.13×10^{-4}	2.22×10^{-5}	1.65×10^{-6}	0.54×10^{-3}
S2	30	-	10.46[1]	1.13×10^{-4}	2.89×10^{-5}	2.06×10^{-6}	0.52×10^{-3}
S3	65	11.31	10.46	2.52×10^{-4}	2.99×10^{-5}	$<2\times10^{-7}$	1.05×10^{-3}
S4	106	11.19	10.38	2.23×10^{-4}	2.77×10^{-5}	6.17×10^{-6}	0.91×10^{-3}
S5	225	11.02	10.27	2.31×10^{-4}	1.40×10^{-5}	4.11×10^{-7}	0.99×10^{-3}

Table 1. Summary of the measured reactive fluid compositions of the experiments performed in the present study. The pH at 60 °C was calculated using PHREEQC together with pH measured at 21 °C and measured reactive fluid compositions. [1]This value was interpolated.

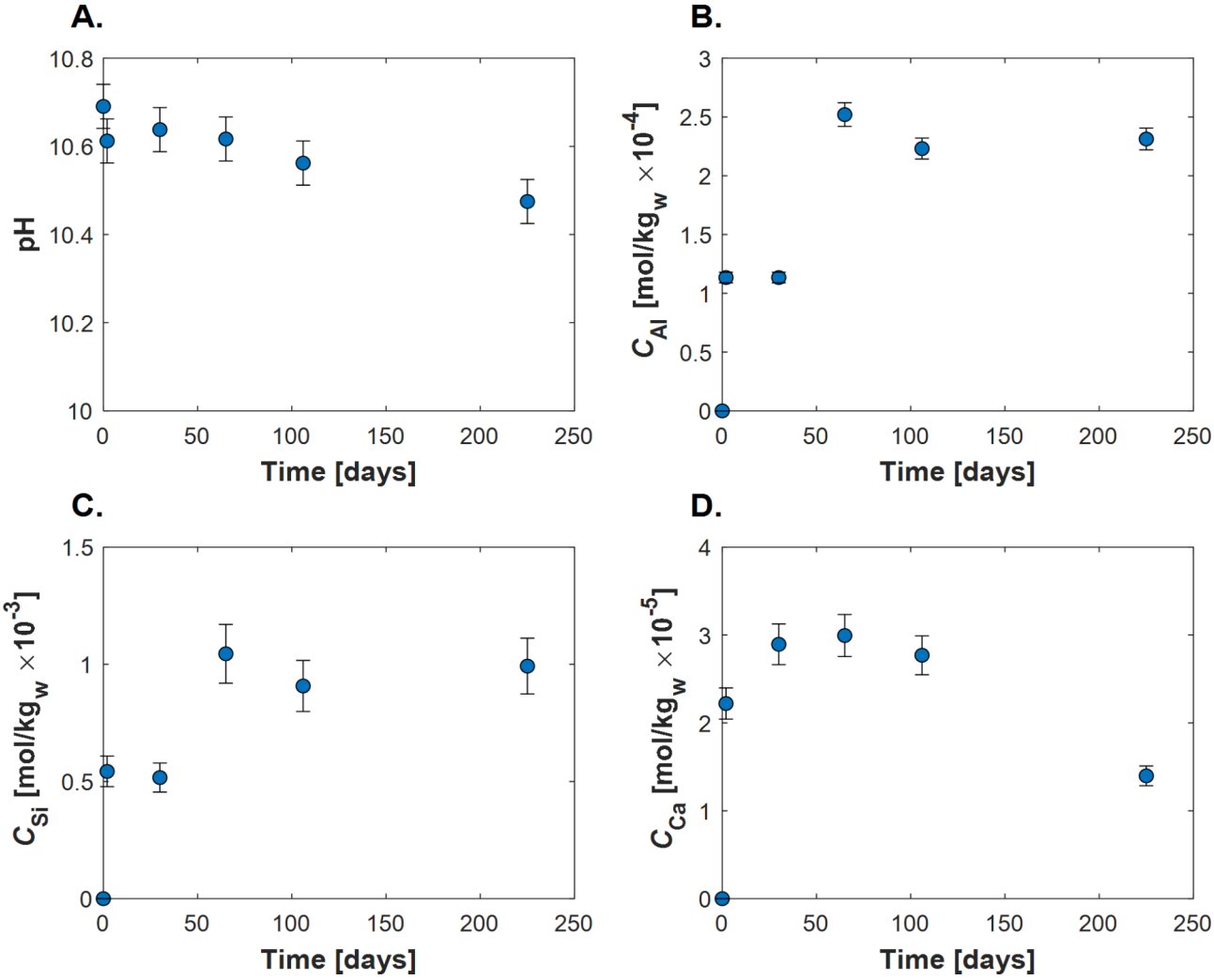

Fig. 2. The temporal evolution of (**A**) in-situ pH, (**B**) dissolved Al concentrations, (**C**) dissolved Si concentrations, and (**D**) Ca concentrations in the aqueous fluids recovered from the individual batch experiments. Measured concentrations have an estimated uncertainty ranging within 4–12%, based on repeated standard solution measurements.

fluids, and Al-hydroxide was close to equilibrium throughout the experiments. Other clay minerals are found to be undersaturated in the reactive fluids.

Analysis of recovered solids

SEM images of the pre- and post-experiment collected from the 2-, 106-, and 225-day batch experiments are shown in Fig. 4. The unreacted stilbite grains had well-defined crystal faces and edges typical of a crystalline mineral. No fine particles or secondary minerals were apparent on these surfaces. The images of post-experiment solids showed the presence of extensive precipitation of secondary minerals on the surfaces of the original stilbite grains as well as the precipitation of isolated precipitates. EDS analysis of these precipitates showed that they are calcium- and carbon-rich. Based on this composition and the observed crystal form, these precipitates were identified as calcite. The stilbite grains remaining after the experiments exhibited extensive fracturing, suggesting that the alteration of this zeolite was heterogeneous and extended deep into the grains. There is no indication of calcite precipitating withing the zeolite itself. Although Mg-saponite clay was supersaturated in the reactive fluids, it was not observed in SEM images of the reacted powder.

The XRD patterns of the initial and reacted solids, as well as reference patterns of stilbite and calcite, are shown in Fig. 5. The XRD patterns of the solids recovered from experiments S3, S4, S5, and the unreacted stilbite sample exhibit peaks consistent with the stilbite reference pattern. Peaks representative of the presence of calcite were not apparent in the reacted solids recovered after the experiments. This could be due to a relatively low concentration of calcite in these samples, as the detection limit of XRD is on the order of 5 volume percent.

The reacted and unreacted solids were analyzed to determine their elemental composition. The compositions of the unreacted stilbite derived from the average of two separate XRF measurements are provided in Table 2. The composition of the unreacted stilbite has an overall average standard deviation of 0.06 mass%. The composition

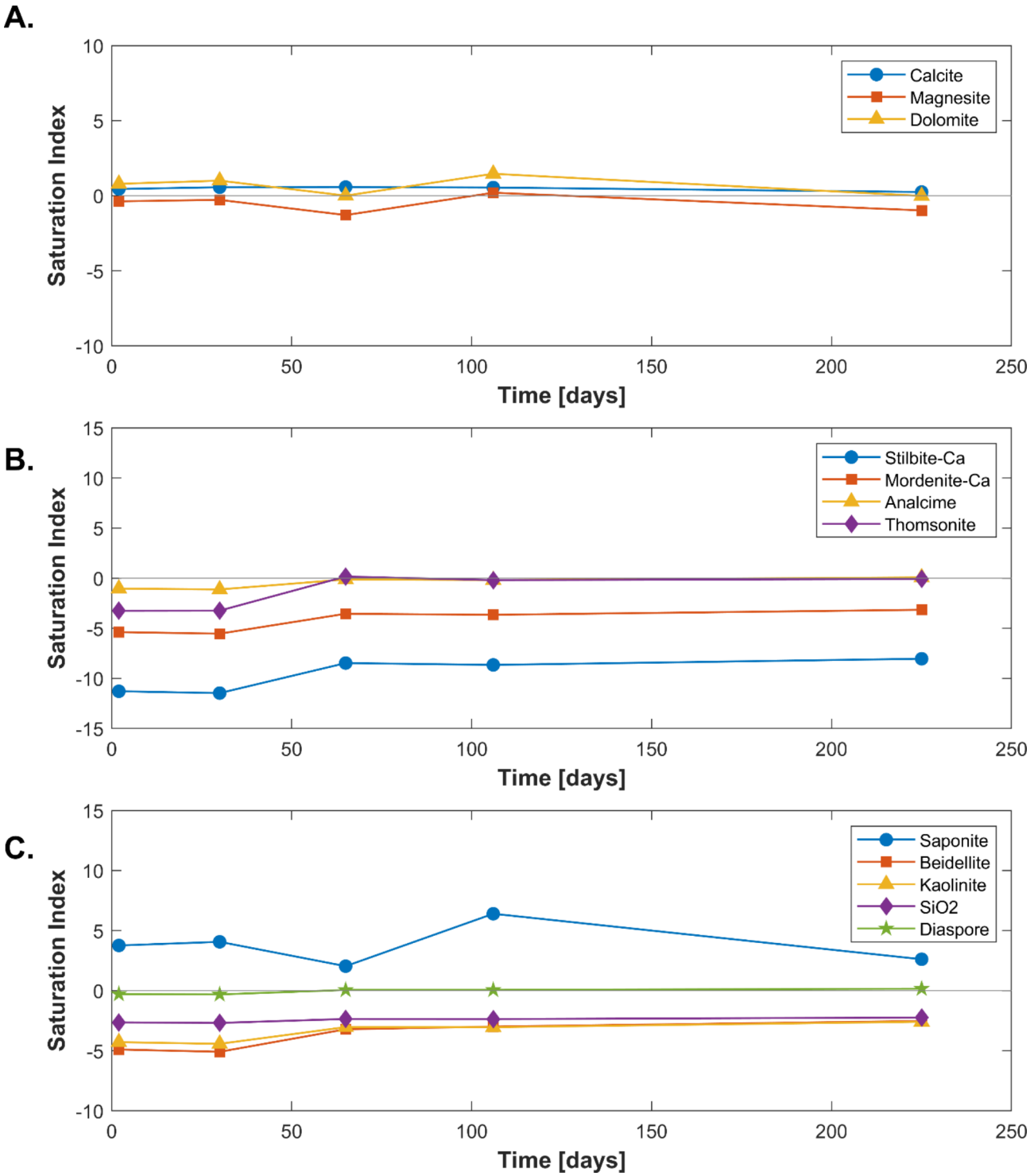

Fig. 3. Temporal evolution of the saturation indices of selected minerals and stilbite in the reactive fluids including (**A**) carbonate minerals, (**B**) stilbite and other zeolites and (**C**) selected clay and Al-hydroxide minerals. These saturation indices were calculated using PHREEQC[50,51] together with its "Kinec.dat" database[43,53]. A positive saturation index indicates the mineral is supersaturated in the fluid, whereas a negative saturation index indicates the mineral is undersaturated in the fluid.

of this unreacted stilbite is close to that reported by Gottardi and Galli[32], Howell et al.[55], and Kiseleva et al.[47]. The water content listed in this table was determined by measuring weight loss after heating the unreacted stilbite sample up to 900 ^{0}C during TGA. The TGA plot is provided in the appendix.

The molar formula of the initial stilbite used in our experiments normalized to 18 O atoms framework is consistent with:

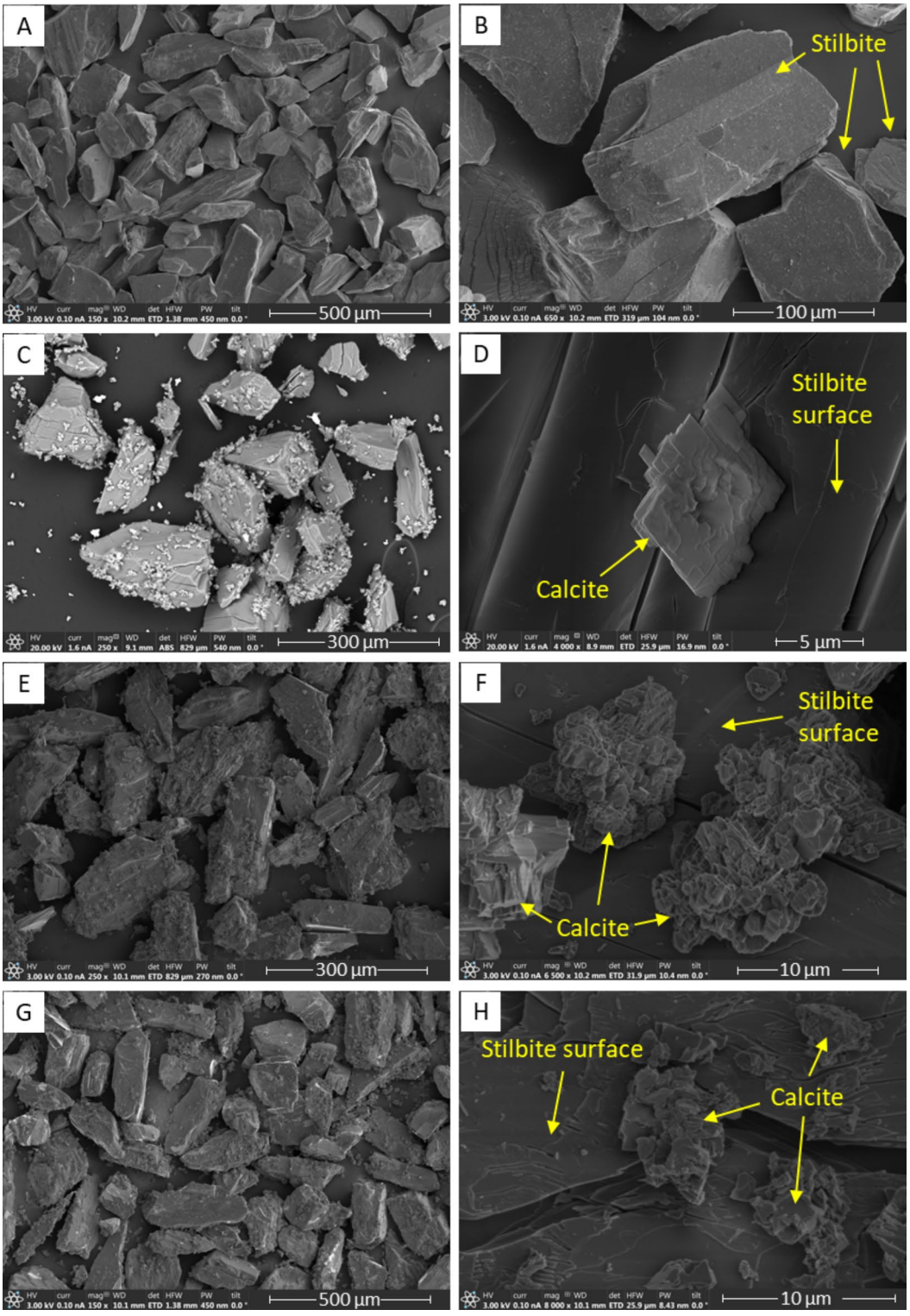

Fig. 4. SEM images of initial and reacted stilbite. (**A**) and (**B**) show natural unreacted stilbite; (**C**) and (**D**) show the solids collected after experiment S1, which lasted two days. (**E**) and (**F**) show solids collected after experiment S4, which lasted 3 months; (**G**) and (**H**) show solids collected after experiment S5, which lasted 7.5 months.

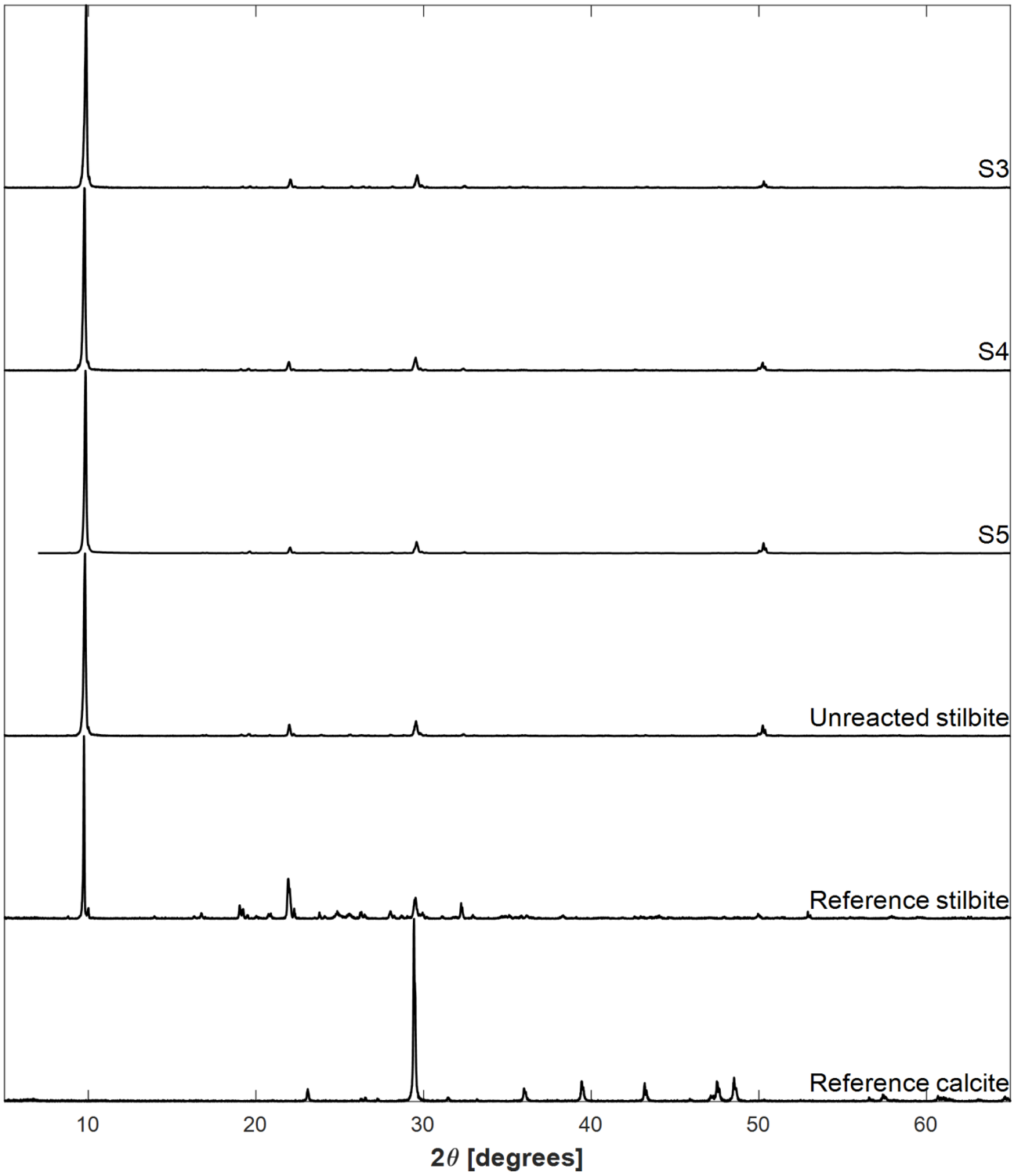

Fig. 5. X-ray diffraction patterns of reacted samples S3, S4, S5, and unreacted stilbite compared with reference patterns of stilbite and calcite taken from the RRUFF database[54].

$$\mathrm{Na_{0.12}Ca\,(Al_{2.12}Si_{6.8})\,O_{18}\cdot 7.5\,(H_2O)} \tag{3}$$

This formula is also in agreement with the compositions of natural stilbite reported in the literature[55], and that adopted in the "kinec.dat" database[43,53] used in geochemical modeling in this study.

Oxide composition [mass %]		Elemental composition [mass%]		Number of atoms or H_2O for 18 framework O atoms	
SiO_2	57.31 ± 0.45	Si	26.79 ± 0.21	Si	6.80
Al_2O_3	15.19 ± 0.06	Al	8.04 ± 0.03	Al	2.12
CaO	7.86 ± 0.05	Ca	5.62 ± 0.04	Ca	1.00
Na_2O	0.51 ± 0.01	Na	0.38 ± 0.006	Na	0.12
H_2O	18.95 ± 0.55	O	40.10 ± 0.81	H_2O	7.51

Table 2. Oxide and elemental composition of the unreacted stilbite determined by XRF.

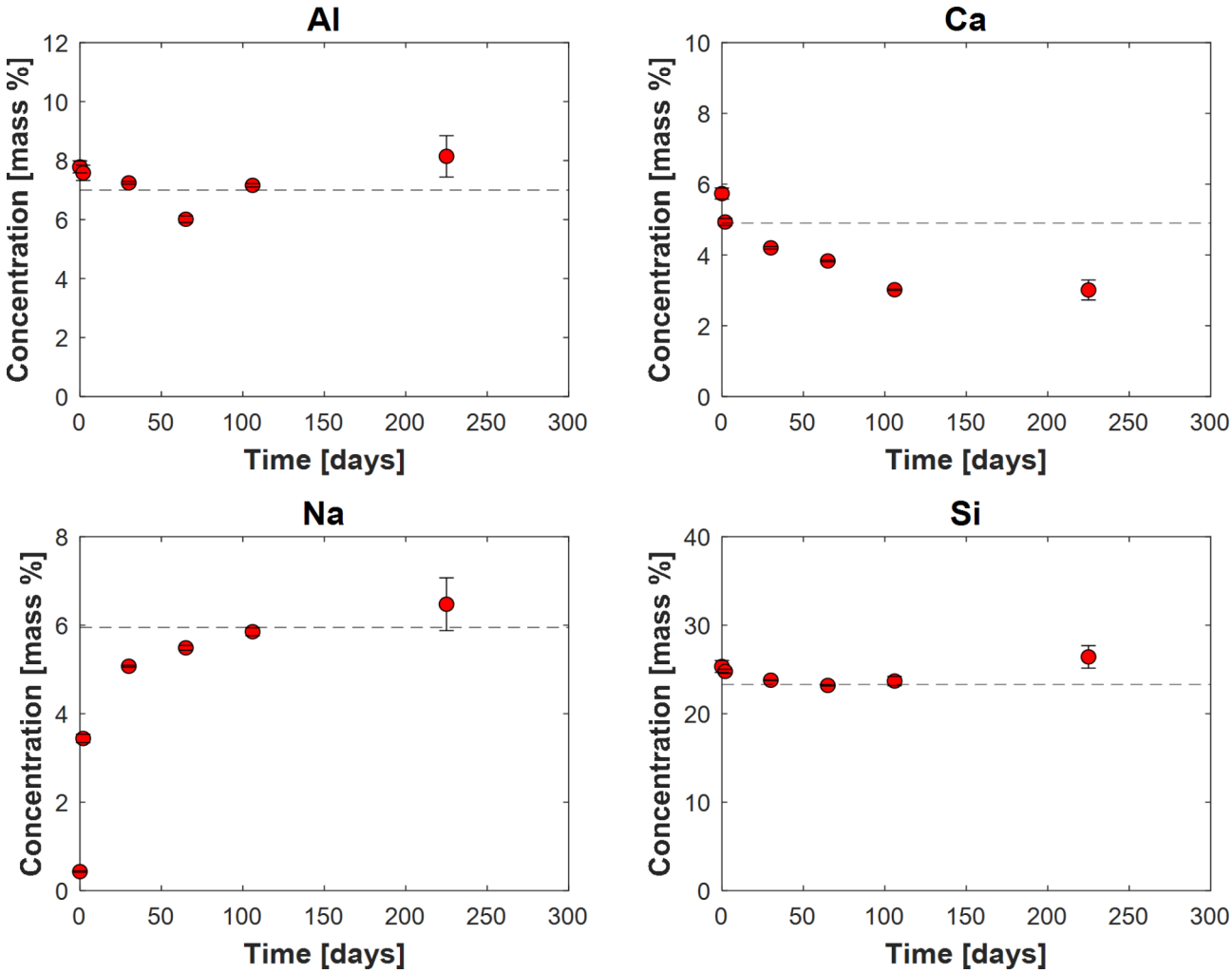

Fig. 6. Temporal evolution of the elemental composition of the solids recovered from the carbonation experiments. Error bars are smaller than data points unless otherwise shown. The dashed horizontal lines in the plots indicate the concentration of these elements if the carbonation reaction had gone to completion in accord with reaction (4) -see text.

Figure 6 shows the elemental composition of the original stilbite and the solids collected after the batch experiments, as determined using ICP-OES. The results are the average of two separate ICP-OES measurements as provided in Table 3; the standard deviations of these values are depicted by the error bars shown in Fig. 6. The initial Na content of the stilbite was 0.4%. This increased to an average of 5.3% in the reacted solids. Consequently, the measured Al, Ca, and Si concentrations of the solids decreased over time. The initial Al content of the stilbite was 8.0%. This decreased to a relative average of 7.2% in the reacted solids, consistent with the added Na mass to the solid. Similarly, the Si content of the stilbite decreased from an initial 27.0% to an average of 24.4% in the reacted solids. The initial Ca content of the stilbite was 5.6%. This decreased to an average of 4.0% in the reacted solids, below that estimated based on the added Na mass. This discrepancy could be due to the use of HF acid

Sample	Elapsed time (days)	Concentration [mass %]				
		Al[1]	Ca[1]	Na[1]	Si[1]	CO_2[2]
S0	0	8.04	5.62	0.38	26.79	0
S1	2	7.58	4.93	3.44	24.78	2.94
S2	30	7.24	4.20	5.07	23.79	4.12
S3	65	6.01	3.83	5.49	23.20	5.06
S4	106	7.16	3.02	5.85	23.69	3.86
S5	225	8.14	3.01	6.47	26.42	3.74
Calculated from reaction (4)	-	7.0	4.89	5.94	23.29	5.37

Table 3. Composition of the initial stilbite, the recovered solids, and of completely carbonated stilbite in accord with reaction (4) – see text. [1]As determined by ICP-OES. [2]As determined from TGA.

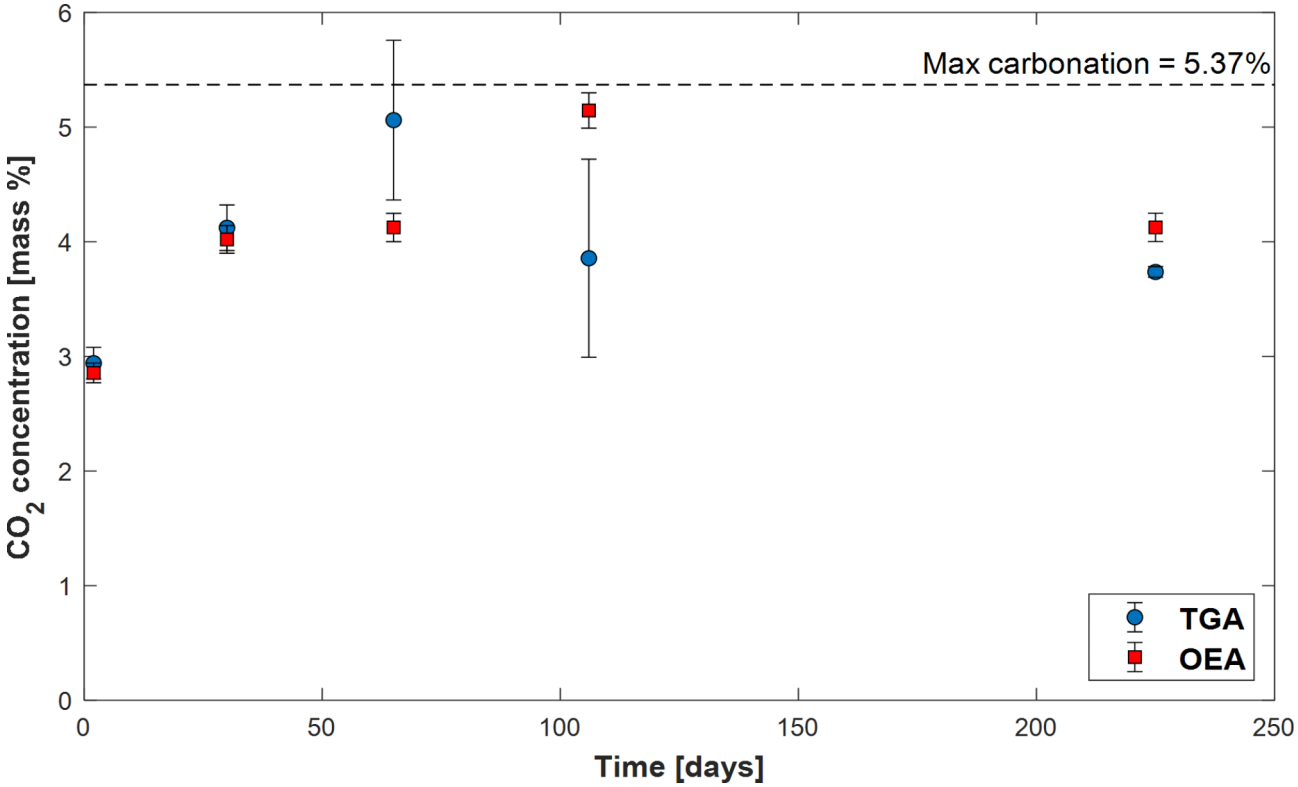

Fig. 7. Mass fraction of CO_2 present in the reacted solids as a function of time, as determined by TGA and OEA. The error bars are smaller than the symbols unless otherwise shown. The differences in the results between the two analytical methods may result from sample heterogeneity. The black dashed line represents the maximum achievable carbonation based on the stoichiometry of reaction (4) – see text.

during sample digestion, which is necessary to dissolve the silicates. However, any excess HF acid could react with Ca from carbonates to form insoluble CaF_2, thereby reducing the measurable Ca concentration[56–58].

Figure 7 illustrates the mass fraction of CO_2 determined by TGA and OEA present in the solids collected after each experiment plotted as a function of experiment duration. The TGA results are derived from two separate measurements to ensure precision and estimate uncertainty. The mass of CO_2 obtained from the two methods are generally consistent with one another. The pre-experiment stilbite sample contains no CO_2. As time progresses and calcite grows due to the stilbite-water interaction, the mass of CO_2 in the reacted solid increases, reaching over 5% CO_2 by mass. Note that there is some minor decrease in the inorganic carbon content of the final collected solid; this is attributed to experimental uncertainty rather than a loss of CO_2 from the solid over time.

Discussion

Efficiency of stilbite carbonation

The efficiency of the stilbite carbonation reaction was evaluated using mass balance considerations. The observations presented above suggest the exchange of Ca for Na in the stilbite structure coupled with the

formation of calcite in accordance with reaction (2). Taking these observations into account, a reaction describing our experiments, assuming all the calcium originally in the stilbite is converted to calcite and the removal of Ca from the stilbite was charged balanced by the addition of Na to this mineral can be written:

$$\underset{\text{Ca-Stilbite}}{Na_{0.12}Ca\left(Al_{2.12}Si_{6.8}\right)O_{18}\cdot 7.5\left(H_2O\right)} + Na_2CO_3 \leftrightarrow \underset{\text{Na-Stilbite}}{Na_{2.12}\left(Al_{2.12}Si_{6.8}\right)O_{18}\cdot 7.5\left(H_2O\right)} + \underset{\text{Calcite}}{CaCO_3} \quad (4)$$

Note that the total masses of Ca, Si, and Al in the reactive fluids are negligible compared to those in the solids. The mass of the solid products on the right side of reaction (4) equals 820 g/mole. In contrast, the molar mass of the unreacted stilbite is 714 g/mole. This mass increase is due to the incorporation of Na and CO_3 into the solid reaction products. It follows that reaction (4) leads to an increased mass of the solids and, therefore, a decrease in the mass percentage of Al, Si, and Ca present in the products compared to the reactants. This is evident in Fig. 6, which shows the mass fraction of Al, Si, Ca, and Na in the pre- and post-experiment solids. Note that the mass fractions consistent with the solids on the right side of reaction (4) are tabulated in Table 3 and marked with dashed lines in Fig. 6. Similarly, the mass fraction of CO_2 of the solid products in reaction (4) after its completion would be 5.37%. It can be seen in Fig. 7 that this value is approached in the solids recovered overtime during the experiments. Taken together, this analysis and the observations presented above strongly suggest that the carbonation of stilbite in our experiments was promoted by the exchange of Na for Ca without otherwise changing the structure of the zeolite. Notably, the structural integrity of the zeolite is preserved during the experiments, as evidenced by the XRD pattern and the SEM images that show the original stilbite remains intact despite observable cracks and etch pits.

The role of mineral exchange reactions in zeolite carbonation

Based on our observations, the stilbite carbonation mechanism is dominated by a Ca for Na exchange process rather than the stoichiometric dissolution of the original stilbite. Mass balance considerations show that most of the calcium originally present in stilbite transformed into calcite within two months, consistent with the near completion of reaction (4). This finding suggests that stilbite carbonation via a cation exchange mechanism occurs more rapidly compared to a mechanism involving the complete dissolution of the original stilbite. The relative rates of stilbite carbonation by cation exchange compared to carbonation by stoichiometric stilbite dissolution can be assessed by mass balance considerations. The formation of calcite from the stoichiometric dissolution of stilbite described by reaction

$$Na_{0.12}Ca\left(Al_{2.12}Si_{6.8}\right)O_{18}\cdot 7.5\left(H_2O\right) \leftrightarrow 0.12Na^{+} + Ca^{2+} + 2.12Al\left(OH\right)_4^{-} + 6.8\ SiO_2\ + 3.26\ H_2O, \quad (5)$$

which when coupled to reaction (2) leads to the overall reaction

$$Na_{0.12}Ca\left(Al_{2.12}Si_{6.8}\right)O_{18}\cdot 7.5\left(H_2O\right) + CO_3^{-2} \leftrightarrow CaCO_3 + 0.12Na^{+} + 2.12Al\left(OH\right)_4^{-} + 6.8\ SiO_2\ + 3.26H_2O \quad (6)$$

In accord with reaction (6), based on the stoichiometric dissolution of stilbite, the number of moles of calcite formed, equal to the number of moles of CO_2 mineralized would be equal to 1/6.8 moles of the SiO_2 released to the aqueous phase. This is assuming no Si bearing secondary phases were formed, such as is the case in our experiments. The mass of CO_2 that would be incorporated into the solids, assuming the dissolution of the zeolite was the rate limiting step, is thus equal to 1/6.8 of the aqueous SiO_2 concentrations measured during our experiments. This mass of CO_2 was calculated taking account of the SiO_2 concentrations presented in Fig. 2. The results of this calculation are shown in Fig. 8. The yellow points in this figure were generated by normalizing the mass of CO_2 calculated to be formed via reaction (6) to the fluid to mass ratio in our reactors. The carbonation by the observed cation exchange mechanism is more than two orders of magnitude faster than if it were controlled by the stoichiometric dissolution of the stilbite. The rapid carbonation rates observed in this study thereby illustrate the potential for exchange reactions to provide a rapid pathway for storing CO_2 in stable carbonate minerals[23].

It is of interest to note that the dissolution of stilbite, as quantified by the mass of Si released to the reactive fluid as illustrated in Fig. 2, appears to stop after 50 days of elapsed time. This coincides with the reactive fluid's attainment of equilibrium with numerous Na zeolite phases in these experiments as shown in Fig. 3. Note that no thermodynamic properties are available for Na-stilbite. Nevertheless, on the basis of the reactive fluid attainment of equilibrium with numerous Na-zeolite phases, we attribute the arresting of zeolite dissolution in our experiments to reactive fluid-Na-stilbite equilibrium, where the Na-stilbite was formed by exchange reactions during our experiments.

Implications for subsurface mineral storage

The findings from this study demonstrate the potential for zeolites to promote the rapid carbonation of water-dissolved CO_2. Notably, we observed the significant carbonation of CO_2 in the presence of ground stilbite, a common zeolite, within two days at 60 °C and in the presence of a 0.1 mol/kg Na_2CO_3 aqueous solution. This remarkably fast carbonation rate is attributed to the rapid release of Ca to the aqueous solution by cation exchange reactions. It can, therefore, be anticipated that carbon disposal through mineral carbonation could be equally accelerated in the subsurface into locations where minerals having large quantities of exchangeable

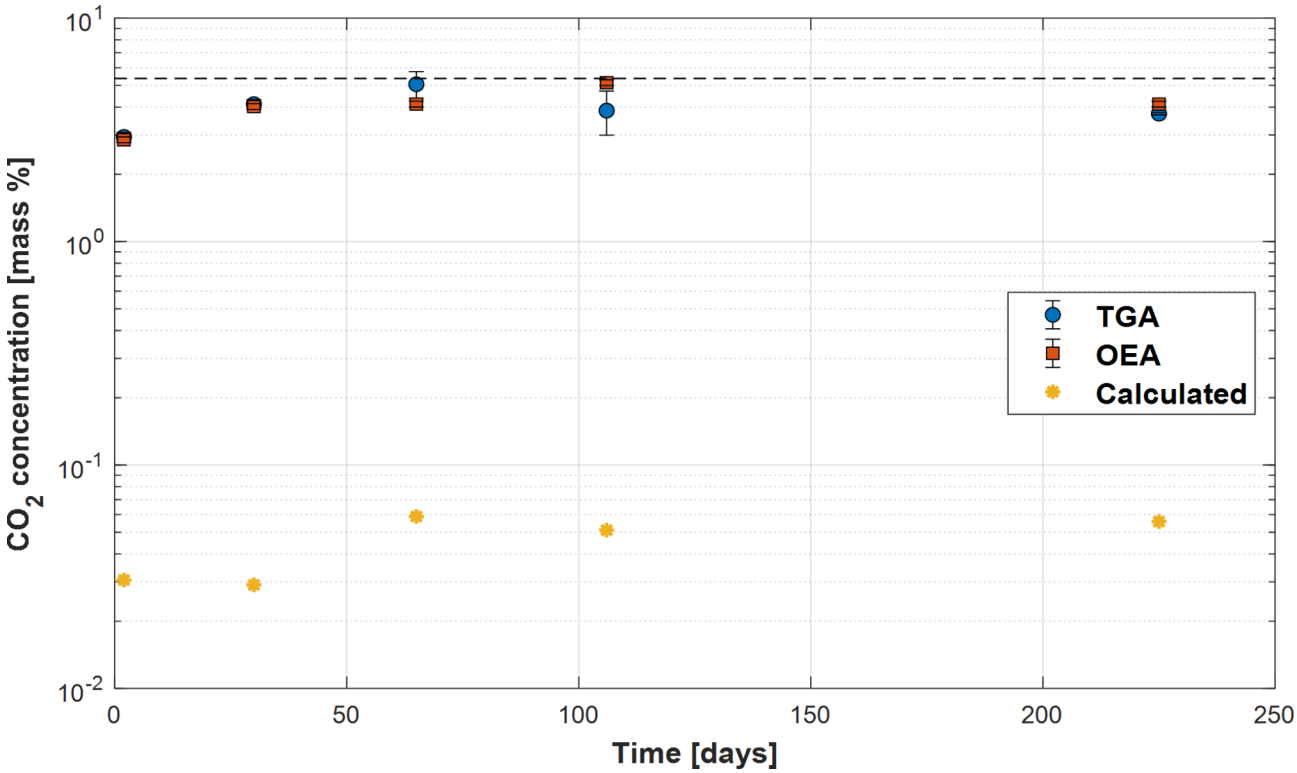

Fig. 8. CO_2 concentration of the recovered solids compared with the mass of CO_2 carbonated over time if the rates were controlled by the stoichiometric dissolution of stilbite. The blue symbols represent CO_2 concentration measured by TGA, the red symbols represent measurements by OEA, and the yellow symbols illustrate mass percent of CO_2 in the recovered solids if it were controlled by the stoichiometric dissolution of the original stilbite– see text. Note the solid dashed line in the figure show the maximum possible CO_2 concentration in the reacted solids in accord with reaction (4).

calcium cations are present if conditions are met to promote the replacement of Ca by aqueous cations in the mineral structures. Note the degree to which Ca is released from zeolites due to exchange reactions likely depends strongly on the aqueous fluid composition. In our study, this exchange was promoted by the presence of aqueous Na in the reactive fluids.

Zeolite minerals, including heulandite and laumontite, are common in basalts that have been altered at temperatures < 200 °C (e.g[59]). Such zeolites tend to form along the preferential water flow paths and in open pore spaces and are Ca-rich. Minerals located in these positions are particularly accessible to injected CO_2-rich fluids and may have the potential for more rapid and more efficient carbon disposal via relatively rapid cation exchange-promoted mechanisms. It should be emphasized, however, that the present study focused on a single aqueous fluid composition in what is largely a proof-of-concept study. The degree to which the aqueous fluid composition influences this rate has yet to be quantified. Nevertheless, the possibility of rapid subsurface carbonation through cation exchange mechanisms compels the consideration of targeting zeolite-bearing basalts for the more efficient and rapid mineralization of CO_2 injected into the subsurface.

It is also of interest to note that the observed rapid carbonation of stilbite appears to be promoted by the presence of aqueous Na. This observation suggests that injection of seawater-dissolved CO_2 would be a potential method to exploit the rapid carbonation potential of the zeolites. The use of seawater-dissolved CO_2 for subsurface carbon storage has the advantage of not using limited freshwater resources. The carbonation of basalt by CO_2-charged seawater has been demonstrated in the laboratory by Voigt et al.[60].

It is anticipated, however, that in contrast to the potential of the mechanism to accelerate CO_2 mineralization in the subsurface, the process will be inefficient for ex-situ mineralization, such as the addition of ground zeolite to the oceans, for several reasons. First, the maximum mass of CO_2 removed by zeolite carbonation is limited by its Ca content, which is relatively low compared to other minerals such as anorthite. Second, Na for Ca exchange in zeolites, such as presented in this study does not increase the alkalinity of the fluid phase. These limitations are, however, overcome in the subsurface, as in-situ does not require the mining and transport of reactive solids, and the presence of other minerals could provide the alkalinity assuring efficient carbonate mineral precipitation.

Conclusions

This study demonstrated the existence of a heretofore overlooked rapid mineral carbonation mechanism by the liberation of Ca from the zeolite, stilbite, by its exchange with aqueous Na. This result suggests that basalts altered to the zeolite facies could achieve carbonation rates comparable to, or even exceeding, those of unaltered basaltic

rocks. The realization of this capability, however, requires a detailed and quantified description of Ca exchange reactions in zeolites as a function of temperature, pH, and aqueous fluid composition. Such information would enable optimization of this rapid cation exchange mechanism in subsurface storage systems.

This study also demonstrated that exchange reactions could substantially influence the rate and extent of subsurface mineral carbon storage efforts. Numerous minerals other than zeolites can rapidly exchange cations, including clays and potentially Ca-rich feldspars, under some conditions. It follows that the accurate modeling of the fate of CO_2 injected into the subsurface as part of mineral storage efforts requires careful consideration of the role of exchange reactions.

Published online: 06 January 2025

Data availability

The fluids and solids composition data and carbonation data have been included in tabular form as part of the main article. The X-ray diffraction (XRD) and the thermogravimetric analysis (TGA) data have been included as part of the Supplementary Information. The PHREEQC code for the Saturation Index (SI) calculations and the SI results are also available in the supplementary information. The database 'kinec.dat' used for carrying out the Saturation Index (SI) calculations is publicly available at https://doi.org/10.1016/j.chemgeo.2023.121632.

References

1. Bachu, S., Gunter, W. D. & Perkins, E. H. Aquifer disposal of CO_2: Hydrodynamic and mineral trapping. *Energy Convers. Manag.* **35**, 269–279 (1994).
2. Lackner, K. S. A guide to CO_2 sequestration. *Science* **300**, 1677–1678 (2003).
3. Oelkers, E. H. & Schott, J. Geochemical aspects of CO_2 sequestration. *Chem. Geol.* **217**, 183–186 (2005).
4. Oelkers, E. H., Gislason, S. R. & Matter, J. Mineral carbonation of CO_2. *Elements* **4**, 333–337 (2008).
5. Gislason, S. R. & Oelkers, E. H. Carbon storage in basalt. *Science* **344**, 373–374 (2014).
6. Campbell, J. S. *et al. Measurements in Geochemical Carbon Dioxide Removal* (Heriot-Watt University, 2023). https://doi.org/10.17861/2GE7-RE08.
7. Addassi, M., Hoteit, H. & Oelkers, E. The impact of secondary silicate mineral precipitation kinetics on CO_2 mineral storage. *SSRN Scholarly Paper* https://doi.org/10.2139/ssrn.4519654 (2023).
8. Oelkers, E. H. & Gislason, S. R. Carbon capture and storage: from global cycles to global solutions. *Geochem. Perspect.* **12**, 179–180 (2023).
9. Metz, B., Davidson, O., Coninck, H. C. de, Loos, M. & Meyer, L. *IPCC Special Report on Carbon Dioxide Capture and Storage*. https://www.ipcc.ch/site/assets/uploads/2018/03/srccs_wholereport-1.pdf (Cambridge University Press, 2005).
10. McGrail, B. P. *et al.* Potential for carbon dioxide sequestration in flood basalts. *J. Geophys. Res. Solid Earth* **111** (2006).
11. Gislason, S. R. et al. Mineral sequestration of carbon dioxide in basalt: A pre-injection overview of the CarbFix project. *Int. J. Greenh. Gas Control* **4**, 537–545 (2010).
12. Snæbjörnsdóttir, S. Ó., Gislason, S. R., Galeczka, I. M. & Oelkers, E. H. Reaction path modelling of in-situ mineralisation of CO_2 at the CarbFix site at Hellisheidi, SW-Iceland. *Geochim. Cosmochim. Acta* **220**, 348–366 (2018).
13. Oelkers, E. H. et al. The subsurface carbonation potential of basaltic rocks from the Jizan region of Southwest Saudi Arabia. *Int. J. Greenh. Gas Control* **120**, 103772 (2022).
14. Hellevang, H. Carbon capture and storage (CCS). in *Petroleum Geoscience: From Sedimentary Environments to Rock Physics* (ed. Bjørlykke, K.) 591–602 (Springer, 2015). https://doi.org/10.1007/978-3-642-34132-8_24.
15. Gadikota, G. Carbon mineralization pathways for carbon capture, storage and utilization. *Commun. Chem.* **4**, 1–5 (2021).
16. Hellevang, H., Aagaard, P., Oelkers, E. H. & Kvamme, B. Can dawsonite permanently trap CO_2?. *Environ. Sci. Technol.* **39**, 8281–8287 (2005).
17. Krevor, S. C. & Lackner, K. S. Enhancing process kinetics for mineral carbon sequestration. *Energy Procedia* **1**, 4867–4871 (2009).
18. Sanna, A., Uibu, M., Caramanna, G., Kuusik, R. & Maroto-Valer, M. M. A review of mineral carbonation technologies to sequester CO_2. *Chem. Soc. Rev.* **43**, 8049–8080 (2014).
19. Kelemen, P. B. et al. Engineered carbon mineralization in ultramafic rocks for CO_2 removal from air: Review and new insights. *Chem. Geol.* **550**, 119628 (2020).
20. Carroll, D. Ion exchange in clays and other minerals. *GSA Bull.* **70**, 749–779 (1959).
21. Kristmannsdottir, H. & Tomasson, J. Zeolite Zones in Geothermal Areas in Iceland (1978).
22. Iijima, A. Geology of natural zeolites and zeolitic rocks. *Pure Appl. Chem.* **52**, 2115–2130 (1980).
23. Alderton, D. Zeolites. in *Encyclopedia of Geology (Second Edition)* (eds. Alderton, D. & Elias, S. A.) 313–325 (Academic Press, 2021). https://doi.org/10.1016/B978-0-08-102908-4.00041-2.
24. Ármannsson, H. 7.12 - Geochemical aspects of geothermal utilization, in *Comprehensive Renewable Energy* (2nd Edition) (ed. Letcher, T. M.) 235–255 (Elsevier, 2022). https://doi.org/10.1016/B978-0-12-819727-1.00166-7.
25. Flanigen, E. M. Chapter 2. Crystal structure and chemistry of natural zeolites, in *Mineralogy and Geology of Natural Zeolites* 19–52 (De Gruyter, 1977). https://doi.org/10.1515/9781501508585-006.
26. Alfredsson, H. A. et al. The geology and water chemistry of the Hellisheidi, SW-Iceland carbon storage site. *Int. J. Greenh. Gas Control* **12**, 399–418 (2013).
27. Sukheswala, R. N., Avasia, R. K. & Gangopadhyay, M. Zeolites and associated secondary minerals in the Deccan Traps of Western India. *Mineral. Mag.* **39**, 658–671 (1974).
28. Slaughter, M. Crystal structure of stilbite. *Am. Mineral.* **55**, 387–397 (1970).
29. Armbruster, T. & Gunter, M. E. Crystal structures of natural zeolites. *Rev. Mineral. Geochem.* **45**, 1–67 (2001).
30. Passaglia, E., Galli, E., Leoni, L. & Rossi, G. The crystal chemistry of stilbites and stellerites. *Bull. Minéralogie* **101**, 368–375 (1978).
31. Lotti, P., Gatta, G. D., Merlini, M. & Liermann, H.-P. High-pressure behavior of synthetic mordenite-Na: An in situ single-crystal synchrotron X-ray diffraction study. *Z. Für Krist. Cryst. Mater.* **230**, 201–211 (2015).
32. Gottardi, G. & Galli, E. Natural zeolites. *Geol. Mag.* **123**, 718 (1985).
33. Moshoeshoe, M., Nadiye-Tabbiruka, M. S. & Obuseng, V. A review of the chemistry, structure, properties and applications of zeolites. *Am. J. Mater. Sci.* **7**, 196–221 (2017).
34. Kumar, S., Srivastava, R. & Koh, J. Utilization of zeolites as CO_2 capturing agents: Advances and future perspectives. *J. CO2 Util.* **41**, 101251 (2020).
35. Boer, D. G., Langerak, J. & Pescarmona, P. P. Zeolites as selective adsorbents for CO_2 separation. *ACS Appl. Energy Mater.* **6**, 2634–2656 (2023).
36. Mumpton, F. A. *Mineralogy and Geology of Natural Zeolites* (De Gruyter, 1977).
37. Drummond, D., De Jonge, A. & Rees, L. V. C. Ion-exchange kinetics in zeolite A. *J. Phys. Chem.* **87**, 1967–1971 (1983).
38. Pabalan, R. T. & Bertetti, F. P. Cation-exchange properties of natural zeolites. *Rev. Mineral. Geochem.* **45**, 453–518 (2001).
39. Ćurković, L., Cerjan-Stefanović, Š & Filipan, T. Metal ion exchange by natural and modified zeolites. *Water Res.* **31**, 1379–1382 (1997).

40. Yang, J., Lee, C.-H. & Chang, J.-W. Separation of hydrogen mixtures by a two-bed pressure swing adsorption process using zeolite 5A. *Ind. Eng. Chem. Res.* **36**, 2789–2798 (1997).
41. Passaglia, E. The heat behaviour of cation exchanged zeolites with the stilbite framework. *Tschermaks Mineral. Petrogr. Mitteilungen* **27**, 67–78 (1980).
42. Cruciani, G., Artioli, G., Gualtieri, A., Stahl, K. & Hanson, J. C. Dehydration dynamics of stilbite using synchrotron X-ray powder diffraction. *Am. Mineral.* **82**, 729–739 (1997).
43. Heřmanská, M., Voigt, M. J., Marieni, C., Declercq, J. & Oelkers, E. H. A comprehensive and consistent mineral dissolution rate database: Part II: Secondary silicate minerals. *Chem. Geol.* **636**, 121632 (2023).
44. Glover, E. T., Faanur, A. & Fianko, J. R. Dissolution kinetics of stilbite at various temperatures under alkaline conditions. *West Afr. J. Appl. Ecol.* **16** (2010).
45. Ragnarsdóttir, K. V. Dissolution kinetics of heulandite at pH 2–12 and 25°C. *Geochim. Cosmochim. Acta* **57**, 2439–2449 (1993).
46. Heřmanská, M., Delerce, S. & Oelkers, E. Can zeolite dissolution promote mineral carbon storage in the subsurface?. *SSRN Scholarly Paper* https://doi.org/10.2139/ssrn.4274266 (2022).
47. Kiseleva, I., Navrotsky, A., Belitsky, I. & Fursenko, B. Thermochemical study of calcium zeolites—heulandite and stilbite. *Am. Mineral.* **86**, 448–455 (2001).
48. Brunauer, S., Emmett, P. H. & Teller, E. Adsorption of gases in multimolecular layers. *J. Am. Chem. Soc.* **60**, 309–319 (1938).
49. Bish, D. & Carey, B. Thermal behavior of natural zeolites. *Reviews in Mineralogy and Geochemistry* **45**, 403–452 (2001).
50. Parkhurst, D. L. & Appelo, C. A. J. *User's Guide to PHREEQC (Version 2): A Computer Program for Speciation, Batch-Reaction, One-Dimensional Transport, and Inverse Geochemical Calculations. Water-Resources Investigations Report* https://pubs.usgs.gov/publication/wri994259 (1999). https://doi.org/10.3133/wri994259.
51. Parkhurst, D. L. & Appelo, C. A. J. Description of input and examples for PHREEQC version 3-A computer program for speciation, batch-reaction, one-dimensional transport, and inverse geochemical calculations. *US Geol. Surv. Tech. Methods* (2013).
52. Voigt, M., Marieni, C., Clark, D. E., Gíslason, S. R. & Oelkers, E. H. Evaluation and refinement of thermodynamic databases for mineral carbonation. *Energy Procedia* **146**, 81–91 (2018).
53. Heřmanská, M., Voigt, M. J., Marieni, C., Declercq, J. & Oelkers, E. H. A comprehensive and internally consistent mineral dissolution rate database: Part I: Primary silicate minerals and glasses. *Chem. Geol.* **597**, 120807 (2022).
54. Stilbite-Ca R050012 - RRUFF Database: Raman, X-ray, Infrared, and Chemistry. https://rruff.info/Stilbite-Ca/R050012.
55. Howell, D. A., Johnson, G. K., Tasker, I. R., O'Hare, P. A. G. & Wise, W. S. Thermodynamic properties of the zeolite stilbite. *Zeolites* **10**, 525–531 (1990).
56. Kemp, A. J. & Brown, C. J. Microwave digestion of carbonate rock samples for chemical analysis. *Analyst* **115**, 1197–1199 (1990).
57. Colodner, D. C., Boyle, E. A. & Edmond, J. M. Determination of rhenium and platinum in natural waters and sediments, and iridium in sediments by flow injection isotope dilution inductively coupled plasma mass spectrometry. *Anal. Chem.* **65**, 1419–1425 (1993).
58. Durand, A. et al. Improved methodology for the microwave digestion of carbonate-rich environmental samples. *Int. J. Environ. Anal. Chem.* **96**, 119–136 (2016).
59. Utada, M. Zeolites in hydrothermally altered rocks. *Rev. Mineral. Geochem.* **45**, 305–322 (2001).
60. Voigt, M. et al. An experimental study of basalt–seawater–CO_2 interaction at 130 °C. *Geochim. Cosmochim. Acta* **308**, 21–41 (2021).

Acknowledgements

The authors thank King Abdullah University of Science and Technology (KAUST) Research Funding Office for supporting this work under Award No. 4357. We thank Dr. Kristján Jónasson, the Curator of Mineralogy and Petrology at the Icelandic Institute of Mineralogy and Petrology, and Sigurdur R. Gislason for their assistance in providing the natural zeolite samples used in this study.

Author contributions

Conceptualization: E.O.; Methodology and Data curation: A.A., M.A., H.H., E.O.; Experiments preparation and execution: A.A., M.A.; Visualization: A.A.; Writing – original draft: A.A.; Writing – review & editing: A.A., M.A., H.H., E.O.; All authors reviewed and approved the manuscript.

Declarations

Competing interests

The authors declare no competing interests.

Additional information

Supplementary Information The online version contains supplementary material available at https://doi.org/10.1038/s41598-024-82520-6.

Correspondence and requests for materials should be addressed to A.A.